IEEE Access
Multidisciplinary ⋮ Rapid Review ⋮ Open Access Journal

Received 28 July 2025, accepted 22 August 2025, date of publication 28 August 2025, date of current version 4 September 2025.

*Digital Object Identifier 10.1109/ACCESS.2025.3603642*

RESEARCH ARTICLE

# Energy-Efficient Resource Allocation for Mission-Critical Applications in Underwater Acoustic Networks

**WALID K. HASAN[1], IFTEKHAR AHMAD[1], (Senior Member, IEEE), QUOC VIET PHUNG[1], (Member, IEEE), YUE RONG[2], (Senior Member, IEEE), HAITHAM KHALED[1], AND DARYOUSH HABIBI[1], (Senior Member, IEEE)**

[1]School of Engineering, Edith Cowan University, Perth, WA 6027, Australia
[2]School of Electrical Engineering, Computing and Mathematical Sciences, Curtin University, Bentley, WA 6102, Australia

Corresponding author: Walid K. Hasan (w.hasan@ecu.edu.au)

This work was supported in part by the Department of Jobs, Tourism, Science and Innovation, Defence Science Centre, Australia, under Grant G1007243.

**ABSTRACT** The Internet of Underwater Things (IoUT) has emerged as a vital technological domain, significantly advancing underwater exploration and communication capabilities. At the core of this paradigm is Underwater Acoustic Communication (UAC), which acts as the primary medium for data transmission in underwater environments, including environmental monitoring, security and surveillance, and underwater exploration. Despite its significance, UAC systems face inherent challenges such as limited bandwidth, high signal attenuation, and long propagation delays. These limitations become particularly significant in mission-critical maritime operations, such as warning systems, underwater navigation and control, and diver safety or emergency communications, where timely and reliable data transmission is crucial. Existing resource allocation solutions often fail to adequately optimize limited UAC bandwidth to address the distinct needs of mission-critical applications, making it difficult to ensure reliability and low delays for critical tasks without compromising non-critical performance. This paper introduces a novel resource management scheme to support mission-critical applications in UAC systems, optimizing the acoustic spectrum using Resource Blocks (RBs) with frequency and time division multiplexing. This approach prioritizes mission-critical applications to ensure high reliability and low latency, while also accommodating non-critical applications. We formulate a resource allocation optimization problem based on application type and present a solution. We also introduce a Meta-Heuristic approach designed to efficiently achieve near-optimal solutions while minimizing computational complexity. Simulation results obtained with the DESERT underwater network simulator show that, compared to existing resource management schemes, our approach significantly reduces end-to-end delay and improves throughput for mission critical applications while optimizes transmission power, thus validating the effectiveness of the proposed solution.

**INDEX TERMS** Acoustic communications, resource sharing, mission-critical applications, resource blocks, Internet of Underwater Things.

## I. INTRODUCTION

The Internet of Underwater Things (IoUT) is a groundbreaking framework that is driving major advances in underwater communication systems and exploration technologies [1], [2], [3], [4]. According to the United Nations, over 90% of natural disasters are water-related, including tsunamis and hurricanes. These disasters highlight the critical need for advanced monitoring and communication systems capable of providing early warnings and supporting life-saving

The associate editor coordinating the review of this manuscript and approving it for publication was Yogendra Kumar Prajapati.

interventions [5]. Recent developments have expanded IoUT applications to include critical tasks such as ocean earthquake and tsunami warning, underwater navigation, and the detection of underwater moving targets [6], [7]. These applications require robust and efficient communication mechanisms to ensure their success.

Underwater Acoustic Communication (UAC) systems, recognized as the primary medium for transmitting data in underwater environments, are indispensable for supporting these advanced IoUT operations [8]. The potential for UAC remains vast yet challenging [9]. Acoustic waves, while offering longer transmission distances compared to RF and optical signals in underwater, face inherent limitations, including significant latencies and high bit error rates [10], [11]. These issues stem from the unique underwater environment characterized by the slow speed of sound and restricted bandwidth. Such constraints are particularly problematic for mission critical IoUT applications, which require high reliability, low latency, and precise timeliness. Failure to meet these stringent demands risks ineffective decision-making, errors in control systems, and potentially catastrophic outcomes [12].

Allocating resources in underwater environments demands innovative approaches, given the diverse Quality of Service (QoS) requirements of various applications [13]. Mission critical applications, such as underwater navigation and emergency communication, demand stringent QoS parameters to ensure high reliability and low latency. Moreover, detection and imaging sonars such as sub-bottom profilers [14] and synthetic aperture sonar systems [15], which are commonly used for object detection, seafloor mapping, and operational awareness, generate critical data that also requires timely and reliable transmission, further emphasizing the need for efficient resource allocation. In contrast, non-critical applications, such as environmental monitoring, can tolerate longer delays and lower data rates, making them less resource intensive. Moreover, underwater communication introduces additional complexities, as signal losses increase significantly with both distance and frequency. Allocating suitable frequency bands becomes essential to minimize attenuation and ensure effective transmission over extended distances.

In terrestrial networks, significant progress has been made in resource allocation strategies tailored for mission critical IoT and WSN applications, where rapid and reliable detection of events such as industrial emergencies or fire outbreaks are paramount. For instance. Farag et al. [16] introduced a slot-stealing mechanism that dynamically reallocates time slots from non-critical to critical data transmissions, ensuring the timely delivery of high-priority information. Moreover, Sakya and Sharma [17] designed a protocol that dynamically adjusts node duty cycles based on current energy levels and traffic conditions, giving precedence to nodes with greater energy availability and larger data queues. Although these strategies work well in terrestrial environments, they depend on structured frameworks that require nodes to connect with a central access point for slot allocation and transmission prioritization. However, these approaches become problematic in underwater environments, dynamic conditions, and high propagation delays disrupt slot synchronization and priority management. These challenges significantly hinder the ability to achieve the real-time responsiveness necessary for mission-critical applications in underwater networks [18].

In the context of underwater networks, existing literature has predominantly focused on developing resource allocation mechanisms aimed at ensuring fair distribution as seen in works such as [19], [20], and [21], or minimizing collisions during data transmission, particularly in scenarios involving spatial-temporal uncertainty [22], [23] and hidden terminal issues [24], [25]. However, these approaches often fail to address the specific needs of mission-critical applications, leaving significant challenges with priority. Moreover, the limited standardization of underwater communication protocols, including notable contributions such as JANUS [26] and PHORCYS [27] developed by the North Atlantic Treaty Organization (NATO), further complicates these issues. While these protocols provide foundational frameworks and utilize Carrier Sense Multiple Access with Collision Avoidance (CSMA/CA) for resource allocation, their susceptibility to channel collisions and reduced throughput underscores the need for more robust solutions tailored to mission-critical underwater communication scenarios.

Therefore, the challenge of implementing priority-based resource allocation between nodes remains largely unexplored, leaving a significant gap in addressing the diverse demands of mission-critical and non-critical application scenarios. Addressing these limitations requires further advancements in resource allocation strategies to enhance the reliability and efficiency of underwater communication frameworks.

To address these challenges, advanced resource allocation strategies and robust communication frameworks are essential for optimizing performance and ensuring reliable data delivery for both mission-critical and non-critical IoUT applications. In this paper, we leverage the concept of Resource Blocks (RBs) and propose a resource allocation solution in UAC. We utilize a hybrid approach that integrates frequency and time division techniques to represent $RB_S$. Our research focuses on optimizing the limited resources of the underwater acoustic channel by allocating resources to nodes based on priority and application type. This ensures that mission-critical applications receive more resources to effectively accomplish urgent and critical tasks, while non-critical applications receive sufficient resources. Moreover, we employ energy-efficient allocation strategies to enhance spectrum utilization and ensure reliable underwater communication.

The main contributions of this paper are summarized as follows:

1) We introduce a novel approach to managing spectrum acoustic in underwater networks. This approach

prioritizes mission-critical applications for high reliability and low latency while accommodating non-critical applications.
2) We formulate an optimization problem to efficiently allocate resources, considering the unique challenges of underwater communication. Our solution ensures that the allocation meets the specific requirements of various applications.
3) To address the complexity of the optimization problem, we propose a robust meta-heuristic algorithm that achieves near-optimal solutions with significantly reduced computational time.
4) The performance of the proposed solution is evaluated and benchmarked against existing methods using the DESERT Underwater simulation framework [28], focusing on key metrics such as throughput, end-to-end delay, and transmission power. The results demonstrate significant improvements in all these areas, validating the effectiveness of our proposed method.

The rest of the paper is organized as follows: Section II reviews related work on resource allocation strategies for UAC systems. Section III introduces the system model, detailing the architecture and categorization of applications. Section IV describes the mathematical model. Section V outlines the optimization framework, defines the resource-allocation problem, and specifies the associated constraints. Section VI presents a comparative performance evaluation of the proposed approach against existing protocols. Finally, Section VII concludes this paper by summarizing the findings presented throughout the paper.

## II. RELATED WORK

Numerous studies have explored efficient resource allocation strategies to optimize channel access in underwater networks. This section highlights recent advancements that prioritize nodes to enhance network performance. We provide a detailed review of recently published literature on resource optimization protocols, emphasizing their design principles and effectiveness. Additionally, Table 1 contrasts our proposed protocol with the leading alternative approaches, focusing on key attributes such as priority management, support for mission-critical applications as well as energy efficient.

Zhang et al. [29] proposed a Load-Based Time Slot Allocation (LBTSA) protocol that dynamically allocates time slots by prioritizing critical data through contention-free TDMA while assigning less critical data to CSMA/CA. However, high network loads in CSMA/CA risk collisions and delays, with scalability adding slot allocation challenges. Rahman et al. [30] introduced a channel allocation aware protocol to address the triple hidden terminal problem in multi-channel underwater sensor networks by leveraging a novel channel allocation matrix and delay mapping database. The protocol allocates more resources to certain nodes based on their channel conditions and delays mapping. However, updating the channel allocation matrix and delay mapping introduces overhead, which impacts scalability in large underwater networks. Liu et al. proposed dynamic resource allocation protocols for underwater networks. Firstly, Packet-Level Slot Scheduling (PLSS) [31], Transmission slots are allocated according to packet size and propagation delay, with precedence given to nodes nearer the sink to minimize end-to-end latency. Secondly, the work focuses on mobile networks, introducing Adaptive Broadcasting (AB) scheduling for Autonomous Underwater Vehicles (AUVs) [32], which adjusts slot lengths and sequences to handle mobility and dynamic topologies. Similarly, Gue et al. [33] proposed a protocol with Adaptive Scheduling (AS) to allocate time slots dynamically based on packet accumulation, transmission needs, and network conditions. It optimizes slot lengths and sequencing to reduce end-to-end delays and ensure efficient, collision-free communication in mobile underwater networks. While PLSS, AB, and AS protocols ensure efficient scheduling to avoid collisions, they inherently introduce longer delays due to the sequential nature of transmissions. Nodes must wait until the current packet transmission is completed and reaches its destination, which can increase the overall transmission time in a large network. Yang et al. [21] proposed a Traffic Aware (TF) protocol that allocates time slots based on depth-layer traffic load, assigns subchannels to reduce collisions, and uses SINR-based power control with adaptive packet lengths. This approach improves fairness, throughput, and energy efficiency. However, it does not consider data priority levels. Mei et al. proposed the Efficient Distributed (ED) protocol [34] and Dynamic High-Load (DHL) [35] to handle dynamic high-load scenarios according to the anticipated data load, ensuring nodes with higher data requirements are prioritized to reduce delays. Both protocols focus on enhancing efficiency and minimizing delays in high-load underwater networks. However, scalability remains an issue in large or highly dense networks due to increasing complexity and overhead. Yun [36] proposed Underwater Multi-Channel MAC with Cognitive Acoustics (UMAC-CA), which allocates time and frequency resources using fixed schedules and distributed sensing to avoid interference.

**TABLE 1. Summary of existing work on resource allocation in UAC.**

| Protocols | Priority Support | Energy Awareness | Mission-Critical Applications |
|---|---|---|---|
| LBTSA [29] | ✓ | × | × |
| CUMAC-CAM [30] | ✓ | ✓ | × |
| PLSS [31] | ✓ | × | × |
| AB [32] | ✓ | × | × |
| AS [33] | ✓ | × | × |
| TF [21] | × | ✓ | × |
| ED [34] | ✓ | × | × |
| DHL [35] | ✓ | × | × |
| UMAC-CA [36] | × | ✓ | × |
| DC [37] | ✓ | ✓ | × |
| Our Work | ✓ | ✓ | ✓ |

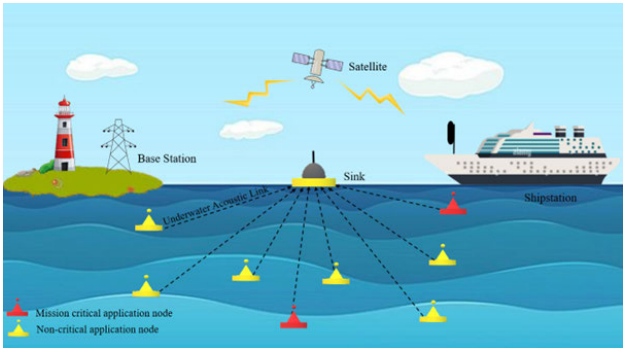


**FIGURE 1.** Network topology architecture.

However, it increases power consumption due to frequent sensing by idle nodes. Zhu et al. [37] proposed a Delay-aware, Collision-free (DC) MAC protocol for underwater networks that uses game theory and cluster-based scheduling. It reduces collisions and energy consumption by dynamically adjusting access probability and prioritizing transmissions based on network topology and delay, resulting in higher throughput and lower end-to-end delay. However, the protocol's performance may degrade in dynamic environments with topology changes.

As Table 1 indicates, although various existing protocols prioritize nodes according to their data demands, they still fall short of meeting the stringent requirements of mission-critical applications. To bridge these gaps, our protocol closes them by dynamically assigning extra RBs to mission-critical traffic, meeting its strict delay and throughput targets while utilizing range-aware, energy-efficient allocation. To our knowledge, it is the first optimization framework expressly tailored to mission-critical workloads in underwater acoustic networks, addressing a previously unfilled research need.

## III. SYSTEM MODEL

### A. SYSTEM ARCHITECTURE

As shown in Figure 1. The system involves the distribution of acoustic nodes in a 3D arrangement with central topology (communication between nodes and sink (Access Point) only, there is no communication between nodes). To facilitate data collection and transmission, Each sensor node receives a unique identifier to enable precise identification and tracking. The surface sink communicates with submerged sensor nodes through an acoustic modem and relays the aggregated data to the base station via an integrated radio modem. Its power supply is provided either by onboard solar panels or through a cabled connection to a proximate support vessel. This power flexibility ensures continuous sink operation and supports the system's communication.

In our established framework, we presume that all sensor nodes are randomly distributed within the communication radius of the sink node. The sink node is positioned at the central point of this defined region. In addition, we opt to exclude any potential variations in node positions brought about by movement. This is due to the negligible nature of such fluctuations when compared to the distances covered within the communication range. This assumption is based on the observation that movements within the network are generally minor relative to the larger scale of communication ranges.

### B. APPLICATION TYPES

Underwater wireless acoustic communication system is designed to provide a wide range of sensors with various applications. Certain applications, such as critical missions, may be negatively affected by traffic management. To adapt to this diversity of applications, the proposed approach considers the following applications,

#### 1) MISSION CRITICAL APPLICATION

This category includes applications that require real-time data transmission without delay. To ensure superior quality and performance, these applications demand increased data rates and ample bandwidth for rapid, low-latency information transmission. Examples include underwater intrusion detection, surveillance, and human activity. Therefore, allocating additional network resources to these applications significantly improves the QoS.

#### 2) NON-CRITICAL APPLICATION

This class covers applications that do not need real-time data transfer, for instance, scientific studies parameters. Such workloads are inherently delay-tolerant, so assigning them fewer network resources has no detrimental impact on their performance or results.

## IV. MATHEMATICAL MODEL

### A. UNDERWATER ACOUSTIC CHANNEL MODEL

UAC channels exhibit distinctive characteristics that affect signal propagation. Unlike typical wireless channels, in UAC channels, the path loss is affected both by distance and signal frequency [38]. Higher frequencies experience more pronounced attenuation due to absorption loss, which intensifies with both frequency and distance, thereby constraining the available bandwidth [39]. Absorption arises from the conversion of acoustic energy into alternative forms of energy, such as heat, during the transmission of the acoustic wave through a medium [40]. This conversion emerges because of interactions between the acoustic wave and the particles or molecules present within the medium. Whereas spreading loss refers to the scattering of energy transmitted by a source as the wavefront propagates across a significant surface area [41]. The shape of the wavefront, spherical or cylindrical, depends on the propagation distance. For extended ranges, cylindrical modeling is used to account for spreading loss, as the propagation is constrained by the sea surface and seabed boundaries. The combined effects of spreading loss and absorption loss contribute to the phenomenon of path loss in UAC. Path loss can be calculated using a mathematical model, which considers factors such as

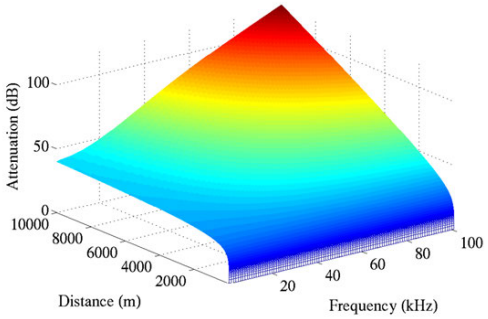


**FIGURE 2.** Influence of frequency and transmission range on acoustic channel attenuation [46].

distance and frequency [42] as shown in (1).

$$A\,(d,f) = A_0 d^k\ \alpha\ (f)^{d_{km}} \tag{1}$$

where $A_0$ is a normalization constant that incorporates baseline losses, $d^k$ is the spread loss over the distance d, k is the spread factor and $\alpha$(f) denotes the acoustic absorption coefficient (dB/km) across a propagation distance expressed in kilometres.

Equation (1) shows that the attenuation in an underwater acoustic channel increases with both propagation distance and signal frequency.

In UAC, overall path loss is typically quantified and reported in decibels (dB) [43].

$$\begin{aligned} 10\log A(d,f) = {} & 10\log A_0 + k\cdot 10\log d \\ & + d_{km}\cdot 10\log a(f). \end{aligned} \tag{2}$$

The absorption coefficient $\alpha$ (f) (in dB per kilometer) is given by Thorp's formula [44], [45] as follows:

$$\alpha(f) = \frac{0.11 f^2}{1+f^2} + \frac{44 f^2}{4100+f^2} + 2.75\times 10^{-4} f^2 + 0.003 \tag{3}$$

The communication range is significantly influenced by the carrier signal frequency. At low frequencies, path loss remains nearly constant over varying distances, whereas at higher frequencies the attenuation coefficient rises sharply, dominating overall path loss and significantly shortening the viable communication range. Figure 2 highlights this relationship, underscoring its importance when choosing a suitable carrier frequency for communication.

The UAC spectrum is subdivided into several frequency bands of equal width (F). Furthermore, the network is divided into three distinct distance tiers. Each tier contains a group of nodes and is assigned one or more dedicated frequency sub-bands from the available spectrum. Accordingly, the following sets are introduced to formalize these divisions.

$\mathrm{F} = [f_1, f_2, f_3, \ldots, f_{|\mathrm{F}|}]$ be the set of all frequency segments,

$\mathrm{R}_n = [\mathrm{S}_R, \mathrm{M}_R, \mathrm{L}_R]$: be the set of distance range.

where

$\mathrm{S}_R$ is short distance range,

$\mathrm{M}_R$ is medium distance range,

$\mathrm{L}_R$ islong distance range,

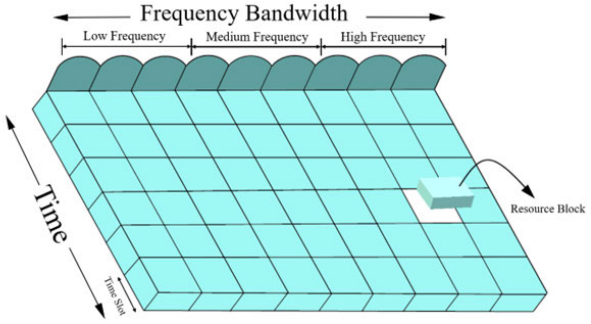


**FIGURE 3.** Resource blocks structure.

$\mathrm{R}_F = [\mathrm{L}_F, \mathrm{M}_F, \mathrm{H}_F]$: denotes the set of frequency ranges. Accordingly, three corresponding subsets, one for each frequency range are specified:

$\mathrm{L}_F = [l_{f_1}, l_{f_2}, l_{f_3}, \ldots, l_{|\mathrm{L_F}|}]$: be the set of channels with low frequencies,

$\mathrm{M}_F = [m_{f_1}, m_{f_2}, m_{f_3}, \ldots, m_{|\mathrm{M_F}|}]$: be the set of channels with medium frequencies,

$\mathrm{H}_F = [h_{f_1}, h_{f_2}, h_{f_3}, \ldots, h_{|\mathrm{H_F}|}]$ be the set of channels with high frequencies.

Efficient channel allocation is pivotal in our model for minimizing attenuation and maximizing spectrum utilization. Accordingly, we define binary decision variables that specify whether each channel is occupied.

$$\alpha_F = \begin{cases} 1, & \text{if all channels in } F \text{ are occupied,} \\ 0, & \text{otherwise.} \end{cases} \tag{4}$$

$$\alpha_{MF} = \begin{cases} 1, & \text{if all channels in } M_F \text{ are occupied,} \\ 0, & \text{otherwise.} \end{cases} \tag{5}$$

$$\alpha_{HF} = \begin{cases} 1, & \text{if all channels in } H_F \text{ are occupied,} \\ 0, & \text{otherwise.} \end{cases} \tag{6}$$

### B. RESOURCE BLOCK MODEL

In our model for UAC, as shown in Figure 3, we combine frequency-division multiplexing (FDM) with time-division multiplexing (TDM). Time is partitioned into T uniform slots, and the pairing of each frequency segment with a time slot yields RB. This method helps us efficiently use the available spectrum by breaking it down into smaller, manageable parts for distribution among various nodes.

Therefore, the aggregate count of RBs for a specific network can be calculated as;

$$|\Xi| = |\mathrm{F}| \times |\mathrm{T}|\,. \tag{7}$$

where $|\Xi|$ denotes the total number RBs on the network, |F| is the the number of frequency and |T| is the number of time slots.

Equation (7) quantifies the network's aggregate capacity, the total number of distinct transmission opportunities. The corresponding sets are defined below.

$\mathrm{T} = [t_1, t_2, t_3, \ldots, t_{|\mathrm{T}|}]$: be the set of all time slots,

$\Xi = \{\xi^{(f,t)} | \ f \in F,\ t \in T\}$: be the set of RBs available for the network,

Moreover, in this research, we categorize applications into two primary types: mission-critical applications and non-critical applications. Consequently, we have defined two corresponding sets of nodes:

$I = [i_1, i_2, i_3, \ldots, i_{|I|}]$: be the set of nodes assigned to mission-critical applications in the underwater network.

$J = [j_1, j_2, j_3, \ldots, j_{|J|}]$: be the set of nodes assigned to non-critical applications in the underwater network.

The total number of active mission-critical and active non-critical nodes is represented by equations (8) and (9), respectively:

$$N_{MCA} = \sum_{i=1}^{|I|} x_i \tag{8}$$

$$N_{NCA} = \sum_{j=1}^{|J|} y_j \tag{9}$$

where $x_i$and $y_j$ are the usage status of a mission-critical and non-critical application node, respectively, corresponding to the following values of the associated binary variables:

$$x_i = \begin{cases} 1, & \text{if node } i \text{ utilize 1 RB or more,} \\ 0, & \text{otherwise.} \end{cases} \tag{10}$$

$$y_j = \begin{cases} 1, & \text{if node } j \text{ utilize 1 RB or more,} \\ 0, & \text{otherwise.} \end{cases} \tag{11}$$

Equations (12) and (13) specify the total number of RBs assigned to mission-critical and non-critical nodes, respectively.

$$RB_c = \sum_{i=1}^{|I|} x_i^{(f,t)} \tag{12}$$

$$RB_{nc} = \sum_{j=1}^{|J|} y_j^{(f,t)} \tag{13}$$

where:

$$x_i^{(f,t)} = \begin{cases} 1, & \text{if } x_i^{(f,t)} \text{ is assigned to node } i, \\ 0, & \text{otherwise.} \end{cases} \tag{14}$$

$$y_j^{(f,t)} = \begin{cases} 1, & \text{if } y_j^{(f,t)} \text{ is assigned to node } j, \\ 0, & \text{otherwise.} \end{cases} \tag{15}$$

The data rate delivered by each RB over a given time duration is ($\lambda^{(f,t)}$) in bits per second is calculated as follows:

$$\lambda^{(f,t)} = \frac{N_b}{|T| \times (\tau + \tau_g)} \tag{16}$$

where:

$N_b$ represents the number of bits carried by each RB.

$\tau$ denotes the length of a single time slot.

$\tau_g$ indicates the guard time separating adjacent time slots.

## V. OPTIMIZATION MODEL

### A. PROBLEM FORMULATION

Our system distinguishes between mission-critical and non-critical applications. Mission-critical nodes necessitate higher data rates or more RBs than non-critical nodes due to their urgent nature and the limited resources available. Our objective is to optimize the utilization of available RBs to support both mission-critical and non-critical application nodes. This requires an allocation strategy that prioritizes mission-critical applications for RB access while ensuring efficient utilization of the remaining RBs for non-critical applications. The optimization problem, along with its objective function and constraints, can then be expressed as follows:

$$Maximize \quad Z = \alpha \sum_{i=1}^{|I|} x_i + \beta \sum_{j=1}^{|J|} y_j \tag{17}$$

$$\sum_{i=1}^{|I|} x_i^{(f,t)} + \sum_{j=1}^{|J|} y_j^{(f,t)} \leq 1, \forall (f,t) \tag{18}$$

$$x_i \leq \sum_{f \in F} \sum_{t \in T} x_i^{(f,t)}, \forall i \in I \tag{19}$$

$$x_i \geq x_i^{(f,t)}, \ \forall i \in I, \forall f \in F, \ \forall t \in T \tag{20}$$

$$y_j \leq \sum_{f \in F} \sum_{t \in T} y_j^{(f,t)}, \forall j \in J \tag{21}$$

$$y_j \geq y_j^{(f,t)}, \ \forall j \in J, \ \forall f \in F, \ \forall t \in T \tag{22}$$

$$\sum_{i=1}^{|I|} \sum_{f \in F} \sum_{t \in T} x_i^{(f,t)} + \sum_{j=1}^{|J|} \sum_{f \in F} \sum_{t \in T} y_j^{(f,t)} \leq |\Xi| \tag{23}$$

$$\sum_{f \in F} \sum_{t \in T} x_i^{(f,t)} \lambda^{(f,t)} \geq d_i, \quad \forall i \in I \tag{24}$$

$$\alpha_F = \left( \sum_{i=1}^{|I|} x_i^{(f,t)} + \sum_{j=1}^{|J|} y_j^{(f,t)} \right), \ \forall f \in F \tag{25}$$

$$\alpha_{M_F} \geq \sum_{f \in M_F} \alpha_f - |M_F| + 1 \tag{26}$$

$$\alpha_{M_F} \leq \alpha_f, \ \forall f \in M_F \tag{27}$$

$$\alpha_{H_F} \geq \sum_{f \in H_F} \alpha_f - |H_F| + 1 \tag{28}$$

$$\alpha_{H_F} \leq \alpha_f, \ \forall f \in H_F \tag{29}$$

$$x_i^{(f,t)} = 0 : \forall i \in L_R, \ \forall f \in \{H_F, M_F\}, \ \forall t \in T \tag{30}$$

$$y_j^{(f,t)} = 0 : \forall j \in L_R, \ \forall f \in \{H_F, M_F\}, \ \forall t \in T \tag{31}$$

$$x_i^{(f,t)} = 0 : \forall i \in M_R, \ \forall f \in \{H_F\}, \ \forall t \in T \tag{32}$$

$$y_j^{(f,t)} = 0 : \forall j \in M_R, \ \forall f \in \{H_F\}, \ \forall t \in T \tag{33}$$

$$x_i^{(f,t)} \leq \alpha_{M_F} : \forall i \in M_R, \ \forall f \in \{L_F\}, \ \forall t \in T \tag{34}$$

$$y_j^{(f,t)} \leq \alpha_{M_F} : \forall j \in M_R, \ \forall f \in \{L_F\}, \ \forall t \in T \tag{35}$$

$$x_i^{(f,t)} \leq \alpha_{H_F} : \forall i \in S_R, \ \forall f \in \{M_F, L_F\}, \ \forall t \in T \tag{36}$$

$$y_j^{(f,t)} \leq \alpha_{H_F} : \forall j \in S_R, \ \forall f \in \{M_F, L_F\}, \ \forall t \in T \tag{37}$$

$$x_i^{(f,t)} \leq \alpha_{M_F} : \forall i \in S_R, \forall f \in \{L_F\}, \ \forall t \in T \tag{38}$$

$$y_j^{(f,t)} \leq \alpha_{M_F} : \forall j \in S_R, \ \forall f \in \{L_F\}, \ \forall t \in T \tag{39}$$

where (17) is the objective function of the optimization problem, which maximizes the number of active node applications (both mission-critical and non-critical) by effectively managing the allocation of the limited RBs in the network. The first summation term in (17) is total mission-critical application nodes weighted by factor $\alpha$, and the second term in (17) is total non-critical application nodes weighted by factor $\beta$. Constraint (18) guarantees no RB is simultaneously assigned to multiple nodes. Additionally, Constraints (19)

through (22) guarantee that a node is designated as active only if it has been assigned at least one RB. Constraint (23) enforces that the cumulative allocation of RBs across both mission-critical and non-critical nodes does not surpass the overall RB capacity of the network. Constraint (24) ensures that each mission-critical node is allocated a sufficient number of RBs to satisfy its required data rate $d_i$. The subsequent constraints are designed to optimize spectrum utilization minimize transmission power and assign suitable frequency bands to each node according to its transmission range, while ensuring efficient monitoring of channel usage across all frequency bands. More specifically, Constraint (25) ensures that the indicator variable $\alpha_F$ is set to 1 only when all channels within the set $F$ are fully occupied. Similarly, constraints (26) and (27) guarantee that $\alpha_{M_F}$ is set to 1 solely when all constituent channels in $M_F$ are allocated. Constraints (28) and (29) ensure that $\alpha_{H_F}$ is activated only when all individual channels within the set $H_F$ are fully occupied.

Constraints (30) and (31) restrict nodes in the $L_R$ region to exclusively use RBs from the low-frequency set $L_F$. Constraints (32) and (33) prohibit nodes within the $R_M$ region from utilizing high-frequency RBs ($H_F$), as these nodes primarily rely on RBs with ($M_F$). If $M_F$ RBs become unavailable, constraints (34) and (35) allow the use of ($L_F$) RBs as an alternative.

Constraints (36) and (37) prioritize RB allocation ($H_F$) to nodes within ($S_R$) region. However, if these RBs are unavailable, ($M_F$) RBs may be used, and ($L_F$) RBs serve as the final fallback option, as specified by constraints (38) and (39).

This optimization problem is formulated as a Binary Integer Programming (BIP) problem [47], which belongs to the class of NP-hard problems. Obtaining an exact solution to this BIP formulation, specifically for constraints (18) through (39), requires solving a combinatorial optimization problem with binary decision variables. We utilized IBM ILOG CPLEX Optimization Studio [48], a robust and efficient tool designed for addressing complex optimization challenges.

### B. META HEURISTIC

While ILOG CPLEX Optimization Studio can provide an exact solution to the problem defined by constraints (18)–(39), the computational cost of doing so is prohibitively high for large-scale scenarios. To mitigate this complexity, we propose a suboptimal yet efficient solution strategy, outlined in Algorithm 1. This method leverages the Whale Optimization Algorithm (WOA) [49], a nature-inspired metaheuristic designed to enhance resource allocation in UAC systems. WOA is modeled after the social behavior of humpback whales, particularly their bubble-net hunting technique, which guides the algorithm's search and exploitation processes.

The algorithm starts by setting up parameters such as population of resource allocation ($\mathbf{Z}_{\mathrm{m}}$), comprising multiple 3D matrices that represent the allocation of RBs across both categories of nodes, F, and T. Other key parameters include the number of iterations and various coefficients including A, (which manages the balance during the optimization of the best-found solution, represented by the matrix ($\mathbf{Z}$) and exploring new solutions), and C, (which adjusts the influence of the target solution on the current solution). In addition, it creates arrays for both categories of nodes, their distances ($R_i$, $R_j$), available frequencies, and time slots. A population of resource allocation, representing potential solutions, is then created.

The algorithm proceeds using a specified number of iterations, updating RBs allocation for each node relative to the best current solution ($\mathbf{Z}$) and constraints allocations (18)-(39). If the allocation adjustment factor ($\|A\| < 1$), the allocation progressively converges toward the most effective solution ($\mathbf{Z}$), simulating an optimization towards the most efficient resource distribution by updating the current solution $\mathbf{Z}_{\mathrm{m}}$, which is based on the matrix ($\mathbf{D}$) that represents the element-wise distance matrix between the current solution $\mathbf{Z}_{\mathrm{m}}$ and the target solution . Otherwise, it adjusts its allocation based on a randomly selected solution ($\mathbf{Z}_{rand}$), mimicking an exploratory search for better resource allocation. The RB allocations are further refined using a spiral equation in 24 (where b shapes the spiral, and l introduces randomness to avoid getting stuck in a local optimum while the solution $\mathbf{Z}_{\mathrm{m}}$ is updated). Algorithm 1 simulates iterative refinement with a probability of less than 0.5. After each update, the efficiency of each resource allocation is recalculated based on the constraints (18)-(39) to identify a best solution ($\mathbf{Z}$). The iteration continues until the maximum number of iterations is reached or a sufficiently optimal solution is found, at which point the algorithm returns the optimal resource allocation strategy ($\mathbf{Z}$), effectively improving resource management and ensuring reliable communication in underwater mission-critical applications.

## VI. PERFORMANCE EVALUATION

This section provides the outcomes of the simulation study conducted to verify and analyze the effectiveness of the proposed methodology. The simulations were conducted using DESERT [28], with our proposed protocol compared against DHL-MAC [35] and LBTSA [29]. DHL-MAC was selected for comparison as it is one of the most recent and relevant centralized protocols. This approach gives priority to nodes with heavier data loads by assigning them additional time slots, thus enhancing overall network throughput. However, it lacks specific mechanisms to accommodate the stringent requirements of mission-critical applications. LBTSA is a hybrid CSMA/TDMA scheme: it schedules urgent traffic using TDMA and non-urgent traffic with CSMA, then switches to a fair allocation mode whenever collisions exceed a defined threshold. Furthermore, we conducted a benchmark with Phorcys, the NATO standard protocol, which employs basic CSMA without any priority differentiation. Other protocols, such as AB [32], PLSS [31] and AS [33],

**TABLE 2. Algorithm 1.**

**Algorithm 1**

**Initialize:** Population size, max iterations, $\tau$, $\tau_g$, $\lambda^{(f,t)}$, $d_i$, $\alpha$, $\beta$.
**Initialize:** $I = [i_1, i_2, i_3, \ldots, i_{|\mathrm{I}|}]$.
**Initialize:** $J = [j_1, j_2, j_3, \ldots, j_{|\mathrm{J}|}]$.
**Initialize:** $R_i = [r_{i1}, r_{i2}, r_{i3}, \ldots, r_{i_{|\mathrm{I}|}}]$.
**Initialize:** $R_j = [r_{j1}, r_{j2}, r_{j3}, \ldots, r_{j_{|\mathrm{J}|}}]$.
**Initialize:** $F = [f_1, f_2, f_3, \ldots, f_{|\mathrm{F}|}]$.
**Initialize:** $T = [t_1, t_2, t_3, \ldots, t_{|\mathrm{T}|}]$.
**Initialize** Resource Allocation Population $\mathbf{Z}_m$ $(m = 1, 2, \ldots, n)$.
**Initialize** $\mathbf{Z}$ as the best solution from $\{\mathbf{Z}_m\}$.
**Initialize:** Coefficients $A$, $C$.
**while** ($k <$ Max number of iterations $(X)$) **do**
  **for each** Resource Allocation $m$ **do**
    Update $A$, $C$.
    **if** $\|A\| < 1$ **then**
      Calculate $D = \left\| C \times \mathbf{Z} - \mathbf{Z}_m \right\|$.
      Update $\mathbf{Z}_m = \mathbf{Z} - A \times D$.
    **else**
      $\mathbf{Z}_{\text{rand}}$ randomly selected from all $\mathbf{Z}_m$.
      Calculate $D = \left\| C \times \mathbf{Z}_{\text{rand}} - \mathbf{Z}_m \right\|$.
      Update $\mathbf{Z}_m = \mathbf{Z}_{\text{rand}} - A \times D$.
    **end if**
    **if** rand $< 0.5$ **then**
      Calculate $D' = \left\| \mathbf{Z} - \mathbf{Z}_m \right\|$.
      Update $\mathbf{Z}_m = D' \times e^{(b \times l)} \times \cos(2\pi l) + \mathbf{Z}$.
    **end if**
    **if** $\mathbf{Z}_m$ does not satisfy constraints (18-39) **go to** 13.
  **end if**
  **end for**
  Update $\mathbf{Z}$ if a better solution is found using (15).
  $k = k + 1$.
**end while**
**Return** $\mathbf{Z}^*$.
**Terminate**.

while incorporating priority mechanisms, exhibit excessively high delays due to their scheduling strategies, making them unsuitable for benchmarking in scenarios requiring low latency. Consequently, these protocols were excluded from the analysis because they have significant limitations regarding mission critical applications requirements.

This study evaluates the proposed protocol against priority-aware schemes like DHL and LBTSA, as well as against Phorcys, the NATO-standard protocol, offering a thorough comparison to demonstrate its effectiveness in meeting the demands of mission-critical underwater applications.

### A. PERFORMANCE METRICS

The simulation evaluates the performance of the three protocols using three primary metrics: throughput, average end-to-end delay, and transmission power consumption, measured separately for critical and non-critical nodes.

#### 1) THROUGHPUT

Throughput is defined as the amount of data successfully received by the sink per unit of time. Several factors can affect throughput, including the data rate of the RB and the overall network traffic load. In our model, all data is received by a single sink. The propagation delay ($P_d$) in UAC requires an effective duration ($E_D$) to be accounted for when calculating throughput for each node. This effective duration considers both the total transmission time and the propagation delay. The $\mathrm{E}_D$ is given by:

$$E_D = \overline{T} - P_d \tag{40}$$

where $\overline{T}$is total simulation duration used to calculate throughput.

Thus, the throughput can be calculated using the following formula:

$$\text{Throughput} = \frac{E_D \times \mathcal{N} \times n_b}{\overline{T} \times |\mathrm{T}| \times (\tau + \tau_g)} \tag{41}$$

where $\mathcal{N}$ is the number of RBs allocated to the node, and $n_b$ is the number of bits per RB that carry the actual data (payload).

#### 2) AVERAGE END-TO-END DELAY

($\overline{D}$) is the total time a data packet takes to travel from the source to the sink node. It includes transmission, propagation, and queuing delays, with guard times accounted for across all three simulated protocols. The average end-to-end delay is computed as follows:

$$\overline{D} = \frac{1}{N_s} \sum\nolimits_{n=1}^{N_s} D_n \tag{42}$$

where $N_s$ is the total number of successfully received packets during the simulation period and $D_n$ represents the end-to-end delay of the $n$-th successfully received packet.

#### 3) AVERAGE TRANSMISSION POWER

($\overline{P}$) We analyze the average transmission power for both categories of application nodes across different protocols. The transmission power required for successful communication is determined based on several factors, including the target Signal-to-Noise Ratio (SNR), the path loss incurred due to propagation range and transmission frequency, and the ambient noise power at the sink.

Assuming a required SNR of 20 dB at the sink, the transmission power for the $n$th successfully transmitted packet is denoted as $P_n$. The average transmission power across all successfully transmitted packets is given by:

$$\overline{P} = \frac{\sum_{n=1}^{N} P_n}{N}. \tag{43}$$

In addition to benchmarking the performance of the proposed protocol against existing solutions such as DHL and TDMA across key evaluation metrics, we further compare our

**TABLE 3. Simulation parameters.**

| Parameter | Value |
|---|---|
| Total bandwidth | 0 – 30 kHz |
| Acoustic speed $S$ | 1500 m/s |
| Bandwidth of each frequency segment $F$ | 5 kHz |
| $\|F\|$ Number of frequency segments | 6 |
| Number of nodes $N$ | 10, 20, 30, 40, 50 |
| Critical: Non-critical ratio | 2:8 |
| $\mathrm{d_i}$ Required data rate for mission-critical applications | 4 kbps |

heuristic-based solution with an optimal solution derived via Integer Linear Programming (ILP) implemented in CPLEX, employing identical evaluation criteria in Subsection F. Moreover, an ablation study is conducted to quantify the performance differences between optimal and suboptimal configurations of the proposed algorithm, using the same set of metrics in Subsection G.

### B. SIMULATION SETTING

Nodes within the underwater network are randomly deployed, subject to the constraint that the average distance for each node category (critical and non-critical) is maintained at 6 km. To maximize resource allocation efficiency for mission-critical applications, the weighting parameters $\alpha$ and $\beta$ in (17) serve to control the relative priority assigned to mission-critical and non-critical applications during resource allocation. In this study, we select $\alpha = 0.9$ and $\beta = 0.1$ to reflect the operational requirements of underwater networks, where mission-critical data must be prioritized to ensure timely and reliable delivery. Increasing $\alpha$ relative to $\beta$ further emphasizes the allocation of resources to mission-critical nodes, resulting in higher throughput and lower latency for critical applications, as observed in our performance results. Conversely, assigning the same weighting factor to both parameters (i.e., $\alpha = \beta$) leads to an equal allocation of resources between critical and non-critical nodes, as discussed in Subsection G. The parameters used in our simulations are detailed in Table 3.

### C. THROUGHPUT

A comparison is provided in Figure 4 of the average total throughput of the four different approaches for critical and non-critical nodes. The results are averaged across five different network scenarios with 10, 20, 30, 40, and 50 nodes. In the case of critical nodes, the proposed protocol outperforms DHL, LBTSA and Phorcys significantly. This illustrates the superior efficiency of the proposed protocol in managing critical nodes and prioritizing their communication requirements effectively. Contrary to this, DHL and LBTSA perform better for non-critical nodes than the proposed protocol. Phorcys consistently yields the lowest average throughput for both critical and non-critical nodes, likely due to its reliance on CSMA, which suffers from high collision rates. Accordingly, the proposed protocol excels at managing critical nodes, but at the cost of non-critical throughput, demonstrating a clear priority strategy.

Figure 5 compares the total throughput for critical nodes across different numbers of nodes for four approaches. The proposed protocol consistently achieves the highest throughput across all node counts. On the other hand, the DHL protocol remains consistent, showing a throughput increase only at higher network node densities. This pattern highlights its comparatively less efficient resource utilization when measured against our proposed approach. In contrast, LBTSA maintains nearly constant low throughput, emphasizing its limitations in handling increased network loads. Phorcys, meanwhile, experiences a decline in total throughput as node density grows, a consequence of excessive RTS/CTS handshakes that aggravate collision rates. The results confirm that the proposed protocol manages critical nodes' network resources more efficiently than DHL, LBTSA and Phorcys. Further, our approach demonstrates robustness and scalability under varying network loads. However, efficiency comes at the cost of limited resources allocated to non-critical nodes because this application is not urgent.

Figure 6 illustrates a comparative analysis of average throughput per node for critical and non-critical data transmissions across various network sizes using protocols that provide priority only: proposed, DHL, and LBTSA. The proposed protocol consistently achieves superior average throughput for critical nodes at all evaluated network sizes, demonstrating its robust capability in dynamically prioritizing mission-critical communications. In contrast, the DHL protocol exhibits delayed prioritization, significantly benefiting critical nodes only when the network size surpasses 40 nodes. Consequently, its critical node throughput remains lower in smaller networks, indicating limited effectiveness for scenarios that necessitate continuous prioritization. LBTSA displays initial prioritization for critical nodes at small network scales (approximately 10 nodes). However, this prioritization diminishes as network size increases due to its hybrid channel access mechanism, transitioning from CSMA to TDMA, thus resulting in comparable throughput between critical and non-critical nodes. The results underscore the proposed protocol's effectiveness in consistently delivering high throughput to critical applications across varying network scales, reinforcing its scalability and resilience under fluctuating network conditions. Nonetheless, this advantage is accompanied by comparatively lower throughput for non-critical nodes, where DHL consistently outperforms our proposed protocol across all network sizes. At the same time, LBTSA surpasses our proposed protocol's non-critical node throughput only at larger network scales once channel contention issues are mitigated through the TDMA mechanism.

### D. END-TO-END DELAY

Figure 7 illustrates a comparative analysis of the average end-to-end delay for mission-critical and non-critical nodes under three communication protocols: Proposed, DHL, LBTSA and

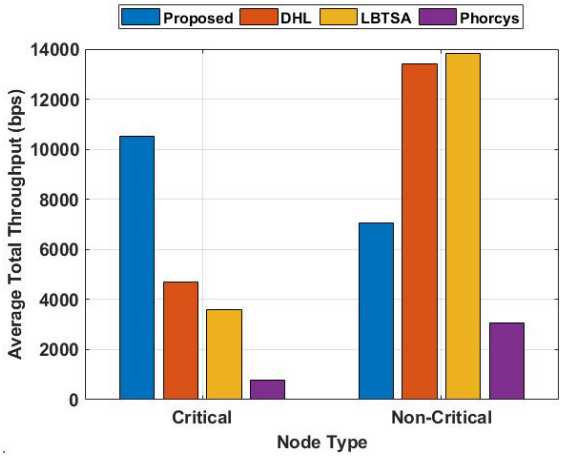


**FIGURE 4.** Average throughput comparison for critical and non-critical nodes (Averaged over networks of 10, 20, 30, 40, and 50 nodes).

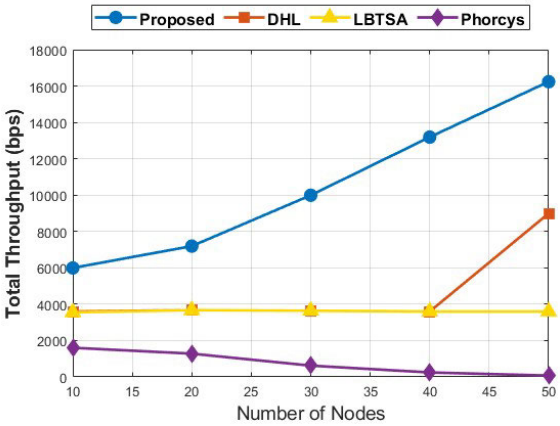


**FIGURE 5.** Critical nodes throughput across different numbers of nodes.

Phorcys. The results are averaged over network scenarios with 10, 20, 30, 40, and 50 nodes.

This highlights that the proposed protocol consistently achieves the lowest average end-to-end delay across all node types and configurations. For mission-critical nodes, the proposed protocol demonstrates a significant reduction in end-to-end delay, achieving approximately 27.41% relative to DHL, by 23.13% relative to LBTSA and by 75.87% to Phorcys. Similarly, for non-critical nodes, the proposed protocol reduces the end-to-end delay by approximately 21% relative to DHL, 16.35% relative to LBTSA and by 73.89% relative to Phorcys. It is clear from this comprehensive analysis that the proposed protocol minimizes end-to-end delays, thereby improving the performance of mission-critical systems.

Figure 8 compares the average end-to-end delay for critical nodes across the Proposed, DHL, LBTSA and Phorcys protocols under varying network sizes, with node counts ranging from 10 to 50. The proposed protocol consistently achieves the lowest end-to-end delay across all tested network densities, highlighting its robustness and ability to maintain low latency for mission-critical applications as the

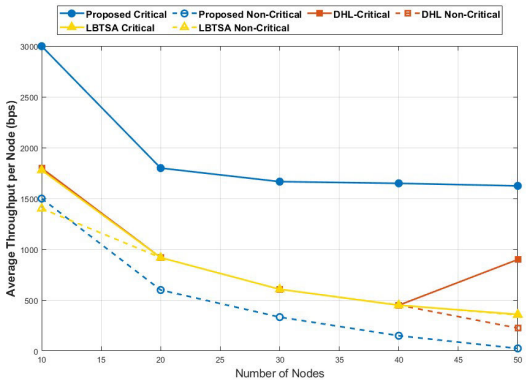


**FIGURE 6.** Analysis of average throughput per node for critical and non-critical nodes across priority protocols.

network scales. The proposed protocol shows significant improvements over DHL, LBTSA and Phorcys in terms of end-to-end delay, where the proposed protocol shows the end-to-end delay reduction of approximately between 13.12% to 36.8% relative to DHL and between 17.72% to 20.3% in comparison to LBTSA and between 31.11% to 84.2% relative to Phorcys. Although the end-to-end delay of the proposed protocol increases slightly as the node count grows from 10 to 50, its rate of increase remains substantially lower than that of the competing schemes.

Figure 9 illustrates the end-to-end delay for critical and non-critical nodes under protocols that provide priority only, Proposed, DHL, and LBTSA protocols. A pronounced and consistent gap between critical and non-critical performance is evident only with our proposed scheme, which maintains both lower and more stable delays for critical traffic as the network size increases. By contrast, DHL only begins to distinguish between critical and non-critical delays once the network exceeds forty nodes, indicating a delayed and limited prioritization effect. LBTSA shows a slight prioritization for critical nodes at ten nodes, but beyond that point, when it reverts to pure TDMA allocation, critical and non-critical delays converge, revealing no sustained clear differentiation.

As a result of these comparisons, the proposed protocol is superior at prioritizing mission-critical communications and managing performance under varying loads. The proposed protocol demonstrates a more effective allocation of resources to critical nodes, where the differentiation between critical and non-critical node delays is more pronounced.

### *E. AVERAGE TRANSMISSION POWER*

In this section, we analyze the average transmission power for critical and non-critical nodes across different protocols. The transmission power for both critical and non-critical nodes is computed, and the results are averaged over network scenarios with 10, 20, 30, 40, and 50 nodes. Figure 10 illustrates the average transmission power of critical and non-critical nodes. The proposed protocol consistently demonstrated the lowest transmission power required for critical nodes and non-critical nodes. Other protocols require higher

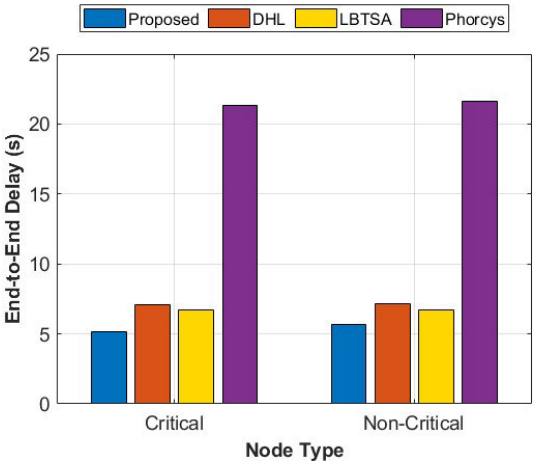


**FIGURE 7.** Average end-to-end delay comparison for critical and non-critical nodes (Averaged over networks of 10, 20, 30, 40, and 50 nodes).

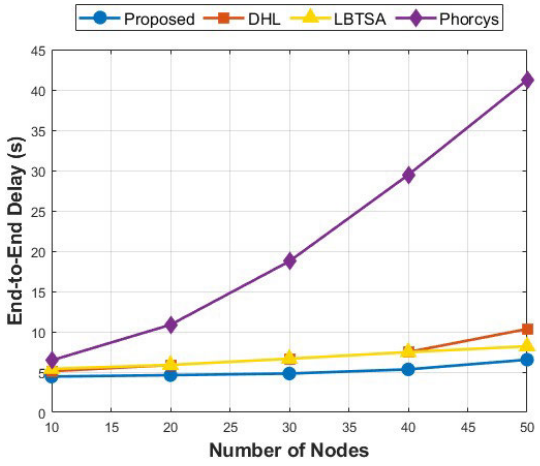


**FIGURE 8.** Critical nodes end-to-end delay across different number of nodes.

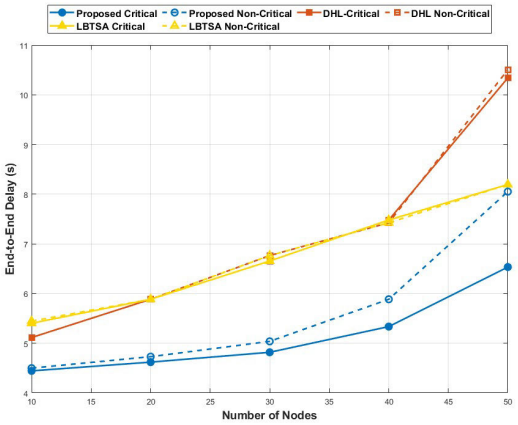


**FIGURE 9.** Analysis of end-to-end delay per node for critical and non-critical nodes across priority protocols.

transmission power than the proposed protocol for critical and non-critical nodes. In particular, Phorcys's reliance on RTS/CTS handshakes and the resulting collisions further elevate its transmission power requirements.

Although both DHL and LBTSA allocate the full bandwidth to each time slot, DHL requires slightly lower transmission power than LBTSA at both critical and non-critical nodes. This difference stems from LBTSA's use of CSMA contention at the beginning of each slot, which increases its overall power expenditure. These results underscore the superior performance of the proposed protocol in required transmission power for both critical and non-critical nodes. The proposed approach efficiently allocates RBs with $H_F$ to near nodes and RBs with $L_F$ to far nodes, optimizing power usage across the network.

### F. META-HEURISTIC SIMULATION RESULTS

This subsection presents a comparison between our heuristic and the ILP solution, generated using CPLEX, in terms of average throughput per node, end-to-end delay, average transmission power and execution time.

Figure 11 shows that the average throughput per node for critical nodes in the Meta-Heuristic solution is approximately 6.6% to 8% lower than the ILP solution. For non-critical nodes, the average throughput per node decreases with the Meta-Heuristic solution, with approximately 6.4 % and 7.8 % reduction compared to the ILP solution.

In Figure 12, the Meta-Heuristic solution in term of end-to-end delay for critical nodes is approximately 6% to 7.5% larger than the ILP solution. For non-critical nodes, the increases in the end-to-end delay of the Meta-Heuristic solution are approximately 6.1% to 7.4% compared to the ILP solution.

Figure 13 presents the average transmission power for both the proposed ILP and Meta-Heuristic solutions, averaged over networks with 10, 20, 30, 40, and 50 nodes. While the figure displays results in dB, the percentage difference in performance is calculated based on power in watts. The results consistently show that the average transmission power of the Meta-Heuristic solution is approximately 7.6% higher than that of the proposed ILP solution for the critical scenario and 7.8% higher for the non-critical scenario when calculated in watts.

Figure 14 shows that the Meta-Heuristic solution consistently outperforms the ILP solution in execution time. While ILP execution time increases sharply with node count, reaching 70 ms at 50 nodes, the Meta-Heuristic approach maintains significantly lower times, with a reduction of approximately 48.6% to 61.5%.

On the other hand, our Meta-Heuristic performs with less execution time than ILP. Therefore, our Meta-Heuristic can be effectively exploited to attain near-optimal results, offering a viable alternative to ILP with potentially reduced computational complexity.

### G. ABLATION STUDIES RESULTS

This ablation study systematically evaluates the impact of relaxing resource allocation constraints and weighting parameters on both mission-critical and non-critical nodes under two distinct scenarios. In the first scenario, resources

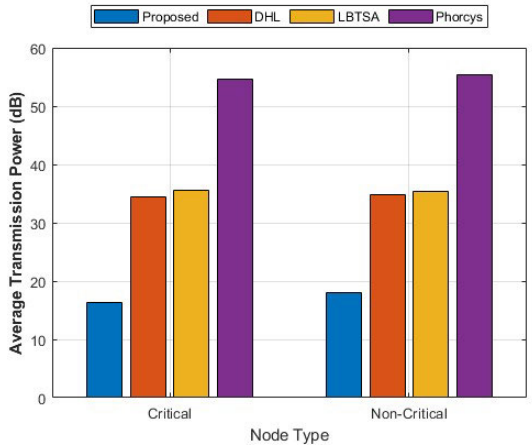


**FIGURE 10.** Average transmission power for critical and non-critical nodes (Averaged over networks with 10, 20, 30, 40, and 50 nodes).

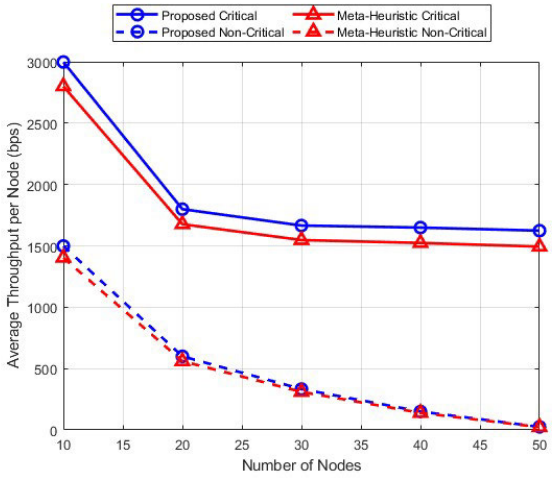


**FIGURE 11.** Average throughput per node across several nodes comparison between the optimum results and our heuristic results.

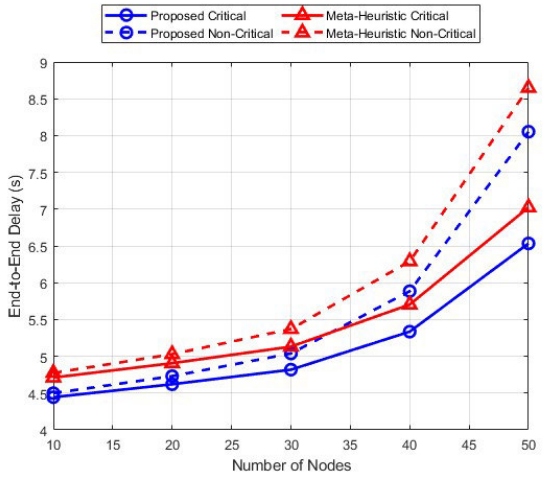


**FIGURE 12.** End-to-end delay across several nodes comparison between the optimum results and our Meta-Heuristic results.

were equally allocated to all nodes with the same weighting parameters (i.e., $\alpha = \beta$). When constraints were relaxed for critical nodes, throughput decreased by 64.2%, and network

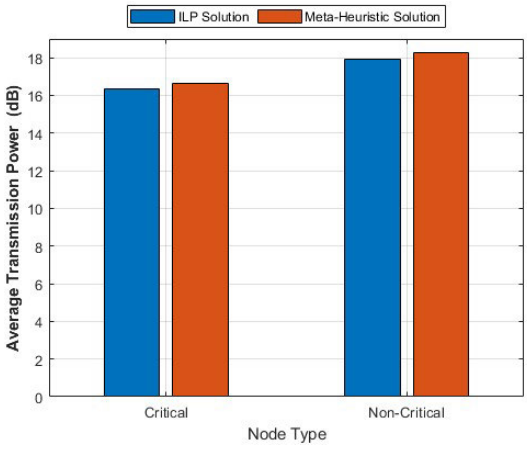


**FIGURE 13.** Average transmission power per node across several nodes comparison between the optimum results and our heuristic results.

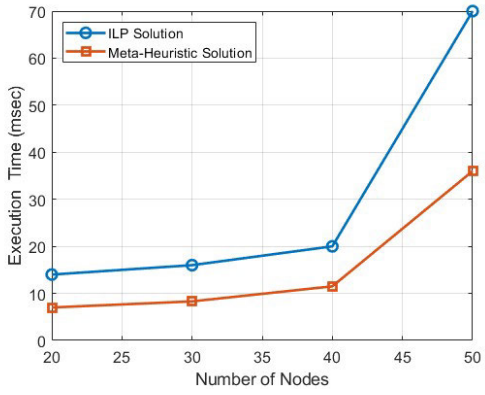


**FIGURE 14.** Execution time comparison between the optimum results and our Meta-Heuristic results.

delay increased by 62.7%. Conversely, non-critical nodes experienced a 67.2% increase in throughput and with latency increased by 61.2% as shown in Figures 15 and 16. In the second scenario, RBs were allocated without consideration of distance or frequency, leading to a substantial increase in average transmission power consumption across both critical and non-critical nodes. Specifically, critical nodes exhibited a sharp escalation in power consumption, rising from 16.34 dB to 62.2 dB, while non-critical nodes experienced a similarly pronounced increase from 17.93 dB to 51.23 dB as illustrated in Figure 17.

These findings reveal that relaxing both constraints benefits non-critical nodes in throughput but severely degrades critical node performance, with both node types facing significant power inefficiencies and increased delays. This emphasizes the need for priority-based and distance-aware resource allocation for our proposed algorithm.

### H. REMARKS AND DISCUSSION

The performance analysis demonstrates that the proposed mechanism, which is based on RB allocation, is significantly better tailored to mission-critical underwater applications

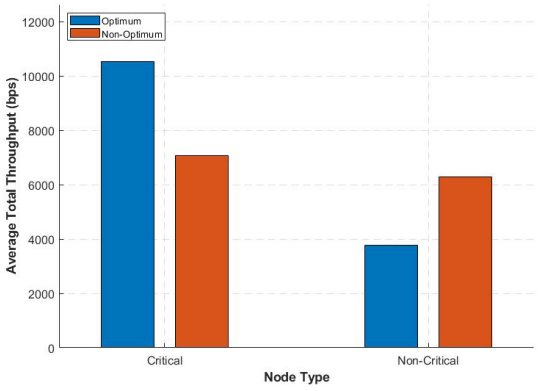


**FIGURE 15.** Average total throughput for optimal and non-optimal configurations of critical and non-critical nodes (Averaged across networks with 10, 20, 30, 40, and 50 nodes).

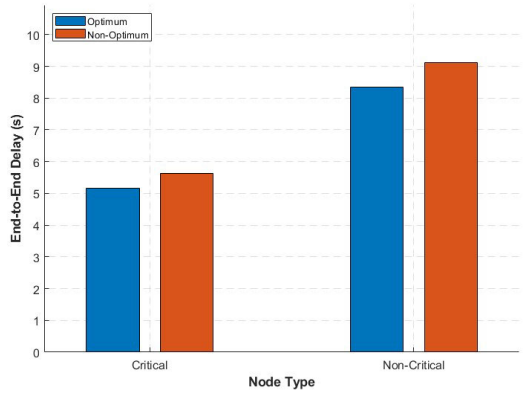


**FIGURE 16.** Average end-to-end delay for optimal and non-optimal configurations of critical and non-critical nodes (Averaged across networks with 10, 20, 30, 40, and 50 nodes).

than the benchmark protocols. By leveraging both frequency and time dimensions, it maximizes the use of the scarce acoustic spectrum and minimizes end-to-end latency and maximizes throughput even as network density rises. This improvement is attributed to the model's prioritization of mission-critical nodes, enabling timely and reliable data delivery for high-priority applications. In contrast, DHL follows a pure TDMA strategy: expanding the frame to accommodate extra slots for critical traffic inevitably lengthens the cycle and, hence, the delay increases. LBTSA is likewise dominated by TDMA and offers no enduring differentiation between critical and non-critical data. Its initial CSMA support for non-critical packets collapses as collisions grow, forcing a reversion to fair allocation by TDMA. Phorcys, which is entirely CSMA-based, performs the worst contention back-offs, repeated RTS/CTS exchanges, and high collision rates inflate latency, throughput and transmission power. Our algorithm dynamically assigns high-frequency RBs to nearby critical nodes and low-frequency RBs to distant nodes, minimizing transmit power while ensuring that mission-critical data reaches the sink swiftly and reliably without draining the limited batteries of underwater sensors. However, the current resource-allocation framework assumes non-mobile nodes, a premise that breaks down in networks

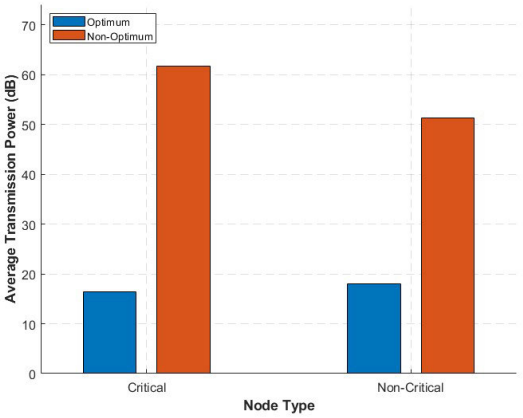


**FIGURE 17.** Average transmission power for optimal and non-optimal configurations of critical and non-critical nodes (Averaged across networks with 10, 20, 30, 40, and 50 nodes).

comprising mobile sensors or AUVs. Mobility introduces Doppler frequency offsets that shift carriers and generate inter-carrier interference between adjacent RBs, thereby suppressing throughput and inflating end-to-end delay. To retain the protocol's efficacy under such conditions, the current mechanism should incorporate adaptive guard bands together with mobility-aware RB reallocation. Concretely, guard intervals must be elastically widened for RBs assigned to rapidly moving nodes and narrowed as their relative motion subsides, mitigating Doppler-induced spectral overlap while preserving overall spectral efficiency.

## VII. CONCLUSION AND FUTURE DIRECTIONS

As the IoUT technology develops rapidly, it has become increasingly important to manage underwater communication resources efficiently. With this expansion of connected systems, there is an increasing need for communication frameworks that are energy-efficient, highly reliable, and capable of supporting high data rates, low latency, and seamless operation in complex and resource-constrained environments. In this paper, an innovative resource allocation framework for UAC is proposed, specifically designed to support mission-critical applications. A proposed framework employs RBs to optimize the limited underwater acoustic spectrum by leveraging frequency and time division multiplexing. This approach prioritizes mission-critical applications to ensure high availability and low latency, while also accommodating non-critical applications. Simulations demonstrate that the proposed framework significantly increases throughput and minimizes end-to-end delays and required transmitted power compared to existing protocols. Furthermore, the implementation of a Meta-Heuristic algorithm achieves near-optimal solutions with reduced complexity, thereby addressing the unique challenges inherent in underwater communications.

Future research will modeling ambient acoustic noise and related impairments. Addressing these factors will require reformulating the optimization problem so that RB allocation and transmission power control are solved jointly under

SINR-based noise constraints to ensure reliable communication. The framework will also be generalized to support mobile nodes, incorporating Doppler-aware RB reassignment and adaptive guard bands to counteract mobility-induced interference.

To enhance adaptability, we plan to fuse multi-modal sensing data with reinforcement-learning (RL) techniques, enabling real-time resource optimization in dynamic underwater environments. Moreover, ecological considerations will be embedded by integrating marine-mammal habitat maps into the allocation policy, thereby facilitating environmentally sensitive and interference-aware RB scheduling that minimizes acoustic impact on vulnerable species.

## ACKNOWLEDGMENT

The authors would like to thank Mohammad Al-Fawa'reh and Muhammad Waqas for their support and guidance throughout the development of this work. Their insights and feedback were crucial in refining the ideas. They deeply appreciate their contributions and encouragement.

## REFERENCES

[1] A. M. Almuhaideb and D. M. Al-Khulaifi, "An efficient authentication and key agreement scheme for the Internet of Underwater Things (IoUT) environment," *IEEE Access*, vol. 12, pp. 175773–175789, 2024.

[2] M. Albekairi, "A comprehensive mutable analytics approach to distinguish sensor data on the Internet of Underwater Things," *IEEE Access*, vol. 12, pp. 95007–95019, 2024.

[3] R. W. L. Coutinho, A. Boukerche, and A. A. F. Loureiro, "A novel opportunistic power controlled routing protocol for Internet of Underwater Things," *Comput. Commun.*, vol. 150, pp. 72–82, Jan. 2020.

[4] M. Jahanbakht, W. Xiang, L. Hanzo, and M. Rahimi Azghadi, "Internet of Underwater Things and big marine data analytics—A comprehensive survey," *IEEE Commun. Surveys Tuts.*, vol. 23, no. 2, pp. 904–956, 2nd Quart., 2021.

[5] United Nations Office for Disaster Risk Reduction (UNDRR), *Better Data for Water-Related Disasters*, Sustainable Development Goals, Jan. 2025].

[6] E. S. Ali, R. A. Saeed, I. K. Eltahir, and O. O. Khalifa, "A systematic review on energy efficiency in the Internet of Underwater Things (IoUT): Recent approaches and research gaps," *J. Netw. Comput. Appl.*, vol. 213, Apr. 2023, Art. no. 103594.

[7] Z. Fang, J. Wang, J. Du, X. Hou, Y. Ren, and Z. Han, "Stochastic optimization-aided energy-efficient information collection in Internet of Underwater Things networks," *IEEE Internet Things J.*, vol. 9, no. 3, pp. 1775–1789, Feb. 2022.

[8] Y. Kang, Y. Su, and Y. Xu, "ACGSOR: Adaptive cooperation-based geographic segmented opportunistic routing for underwater acoustic sensor networks," *Ad Hoc Netw.*, vol. 145, Jun. 2023, Art. no. 103158.

[9] K. Y. Islam, I. Ahmad, D. Habibi, and A. Waqar, "A survey on energy efficiency in underwater wireless communications," *J. Netw. Comput. Appl.*, vol. 198, Feb. 2022, Art. no. 103295.

[10] O. Bello and S. Zeadally, "Internet of Underwater Things communication: Architecture, technologies, research challenges and future opportunities," *Ad Hoc Netw.*, vol. 135, Oct. 2022, Art. no. 102933.

[11] R. Kumar, S. Shekhar, H. Garg, M. Kumar, B. Sharma, and S. Kumar, "EESR: Energy efficient sector-based routing protocol for reliable data communication in UWSNs," *Comput. Commun.*, vol. 192, pp. 268–278, Aug. 2022.

[12] X. Hou, J. Wang, Z. Fang, X. Zhang, S. Song, X. Zhang, and Y. Ren, "Machine-learning-aided mission-critical Internet of Underwater Things," *IEEE Netw.*, vol. 35, no. 4, pp. 160–166, Jul. 2021.

[13] S. Yang, Y. Su, X. Wang, and R. Fan, "Resource allocation for cognitive underwater acoustic downlink OFDMA system with a practical spectrum sensing scheme," *IEEE Internet Things J.*, vol. 11, no. 5, pp. 8731–8745, Mar. 2024.

[14] C. Tan, X. Zhang, P. Yang, and M. Sun, "A novel sub-bottom profiler and signal processor," *Sensors*, vol. 19, no. 22, p. 5052, Nov. 2019, doi: 10.3390/s19225052.

[15] X. Zhang, P. Yang, and D. Cao, "Synthetic aperture image enhancement with near-coinciding nonuniform sampling case," *Comput. Electr. Eng.*, vol. 120, Dec. 2024, Art. no. 109818, doi: 10.1016/j.compeleceng.2024.109818.

[16] H. Farag, M. Gidlund, and P. Osterberg, "A delay-bounded MAC protocol for mission- and time-critical applications in industrial wireless sensor networks," *IEEE Sensors J.*, vol. 18, no. 6, pp. 2607–2616, Mar. 2018.

[17] G. Sakya and V. Sharma, "ADMC-MAC: Energy efficient adaptive MAC protocol for mission critical applications in WSN," *Sustain. Comput., Informat. Syst.*, vol. 23, pp. 21–28, Sep. 2019.

[18] W. K. Hasan, I. Ahmad, D. Habibi, Q. V. Phung, M. Al-Fawa'reh, K. Y. Islam, R. Zaheer, and H. Khaled, "A survey on energy efficient medium access control for acoustic wireless communication networks in underwater environments," *J. Netw. Comput. Appl.*, vol. 235, Mar. 2025, Art. no. 104079.

[19] M. Zheng, W. Ge, X. Han, and J. Yin, "A spatially fair and low conflict medium access control protocol for underwater acoustic networks," *J. Mar. Sci. Eng.*, vol. 11, no. 4, p. 802, Apr. 2023.

[20] W. Zhang, X. Wang, G. Han, Y. Peng, M. Guizani, and J. Sun, "A load-adaptive fair access protocol for MAC in underwater acoustic sensor networks," *J. Netw. Comput. Appl.*, vol. 173, Jan. 2021, Art. no. 102867.

[21] S. Yang, X. Liu, and Y. Su, "A traffic-aware fair MAC protocol for layered data collection oriented underwater acoustic sensor networks," *Remote Sens.*, vol. 15, no. 6, p. 1501, Mar. 2023.

[22] Y. Qiuling, C. Yanxia, D. Wei, L. Tian, Z. Rongxin, and H. Xiangdang, "Cluster-based spatial–temporal MAC scheduling protocol for underwater sensor networks," *IEEE Sensors J.*, vol. 23, no. 15, pp. 17690–17702, Aug. 2023.

[23] X. Liu, X. Du, M. Li, L. Wang, and C. Li, "A MAC protocol of concurrent scheduling based on spatial–temporal uncertainty for underwater sensor networks," *J. Sensors*, vol. 2021, no. 1, Jan. 2021, Art. no. 5558078.

[24] X. Jin, Z. Liu, and K. Ma, "FCFS: A dual-channel and reservation-based MAC protocol for underwater acoustic networks," *IEEE Internet Things J.*, vol. 12, no. 4, pp. 3980–3990, Feb. 2025.

[25] N. Hao, Y. Su, R. Fan, and L. Li, "FDBUL: A delay-aware full-duplex MAC protocol for underwater acoustic sensor networks," *IEEE Sensors J.*, vol. 23, no. 16, pp. 18738–18751, Aug. 2023.

[26] J. Potter, J. Alves, D. Green, G. Zappa, I. Nissen, and K. McCoy, "The Janus underwater communications standard," in *Proc. Underwater Commun. Netw. (UComms)*, Sep. 2014, pp. 1–4.

[27] J. Davies, P. Randall, J. Neasham, B. Sherlock, and A. Hamilton, "Phorcys waveform architecture," in *Proc. 6th Underwater Commun. Netw. Conf. (UComms)*, Aug. 2022, pp. 1–4.

[28] F. Campagnaro, R. Francescon, F. Guerra, F. Favaro, P. Casari, R. Diamant, and M. Zorzi, "The DESERT underwater framework v2: Improved capabilities and extension tools," in *Proc. IEEE 3rd Underwater Commun. Netw. Conf. (UComms)*, Aug. 2016, pp. 1–5.

[29] Z. Zhang, W. Shi, Q. Niu, Y. Guo, J. Wang, and H. Luo, "A load-based hybrid MAC protocol for underwater wireless sensor networks," *IEEE Access*, vol. 7, pp. 104542–104552, 2019.

[30] P. Rahman, A. Karmaker, M. S. Alam, M. A. Hoque, and W. L. Lambert, "CUMAC-CAM: A channel allocation aware MAC protocol for addressing triple hidden terminal problems in multi-channel UWSNs," *Social Netw. Appl. Sci.*, vol. 1, no. 7, p. 805, Jul. 2019.

[31] M. Liu, X. Zhuo, Y. Wei, Y. Wu, and F. Qu, "Packet-level slot scheduling MAC protocol in underwater acoustic sensor networks," *IEEE Internet Things J.*, vol. 8, no. 11, pp. 8990–9004, Jun. 2021.

[32] M. Liu, X. Zhuo, Y. Yuan, Y. Lu, Y. Wei, X. Tu, and F. Qu, "Adaptive scheduling MAC protocol in underwater acoustic broadcast communications for AUV formation," *IEEE Internet Things J.*, vol. 10, no. 8, pp. 6887–6901, Apr. 2023.

[33] J. Guo, S. Song, J. Liu, M. Pan, J.-H. Cui, and G. Han, "AS-MAC: An adaptive scheduling MAC protocol for reducing the end-to-end delay in AUV-assisted underwater acoustic networks," *IEEE Trans. Mobile Comput.*, vol. 24, no. 2, pp. 1197–1211, Feb. 2025.

[34] H. Mei, H. Wang, X. Shen, Z. Jiang, W. Bai, C. Wang, and Q. Zhang, "An efficient distributed MAC protocol for underwater acoustic sensor networks," *IEEE Sensors J.*, vol. 23, no. 4, pp. 4267–4284, Feb. 2023.

[35] H. Mei, H. Wang, X. Shen, Z. Jiang, W. Bai, C. Wang, and Q. Zhang, "An adaptive MAC protocol for underwater acoustic sensor networks with dynamic-high load," *IEEE Sensors J.*, vol. 24, no. 6, pp. 9059–9072, Mar. 2024.
[36] C. Yun, "Underwater multi-channel MAC with cognitive acoustics for distributed underwater acoustic networks," *Sensors*, vol. 24, no. 10, p. 3027, May 2024.
[37] R. Zhu, L. Liu, P. Li, N. Chen, L. Feng, and Q. Yang, "DC-MAC: A delay-aware and collision-free MAC protocol based on game theory for underwater wireless sensor networks," *IEEE Sensors J.*, vol. 24, no. 5, pp. 6930–6941, Mar. 2024.
[38] N. Morozs, W. Gorma, B. T. Henson, L. Shen, P. D. Mitchell, and Y. V. Zakharov, "Channel modeling for underwater acoustic network simulation," *IEEE Access*, vol. 8, pp. 136151–136175, 2020.
[39] M. Stojanovic and J. Preisig, "Underwater acoustic communication channels: Propagation models and statistical characterization," *IEEE Commun. Mag.*, vol. 47, no. 1, pp. 84–89, Jan. 2009.
[40] Y. Sun, X. Yuan, Z. Jin, G. Hong, M. Chen, M. Zhou, W. Li, and D. Fang, "An effective method to enhance the underwater sound absorption performance by constructing a membrane-type acoustic metamaterial," *J. Phys. D, Appl. Phys.*, vol. 55, no. 43, Oct. 2022, Art. no. 435302.
[41] A. Toky, R. P. Singh, and S. Das, "Localization schemes for underwater acoustic sensor networks—A review," *Comput. Sci. Rev.*, vol. 37, Aug. 2020, Art. no. 100241.
[42] K. Saraswathi, K. Netravathi, and S. Ravishankar, "A study on channel modeling of underwater acoustic communication," *Int. J. Res. Comput. Commun. Technol.*, vol. 3, no. 1, pp. 143–147, 2014.
[43] S. Han, Y. Noh, R. Liang, R. Chen, Y.-J. Cheng, and M. Gerla, "Evaluation of underwater optical-acoustic hybrid network," *China Commun.*, vol. 11, no. 5, pp. 49–59, May 2014.
[44] W. H. Thorp, "Analytic description of the low-frequency attenuation coefficient," *J. Acoust. Soc. Amer.*, vol. 42, no. 1, p. 270, Jul. 1967.
[45] Y. Lou, N. Ahmed, Y. Lou, N. Ahmed, "UWAC challenges and research trends," in *Underwater Communications and Networks*. Cham, Switzerland: Springer, 2022, pp. 99–115.
[46] C. M. G. Gussen, P. S. R. Diniz, M. L. R. Campos, W. A. Martins, F. M. Costa, and J. N. Gois, "A survey of underwater wireless communication technologies," *J. Commun. Inf. Syst.*, vol. 31, no. 1, pp. 242–255, 2016.
[47] M. Conforti, G. Cornuéjols, and G. Zambelli, "Integer programming models," in *Integer Programming*. Cham, Switzerland: Springer, 2014, pp. 45–84.
[48] *User's, ILOG CPLEX Optimization Studio User's Manual*, vol. 8, Armonk, New York, NY, USA, 2017.
[49] S. Mirjalili and A. Lewis, "The whale optimization algorithm," *Adv. Eng. Softw.*, vol. 95, pp. 51–67, May 2016.

**WALID K. HASAN** received the Bachelor of Electrical and Electronic Engineering degree from Gharyan University, Libya, in 2006, and the Master of Telecommunication and Network Engineering degree from La Trobe University, Australia, in 2012. He is currently pursuing the Ph.D. degree in electrical and electronic engineering with Edith Cowan University, Australia. He has also received a Postgraduate Certificate of Network with Swinburne University, Australia, in 2013. His research areas include underwater wireless communication, the IoT, and computer networks.

**IFTEKHAR AHMAD** (Senior Member, IEEE) received the Ph.D. degree in communication networks from Monash University, Australia, in 2007. He is currently an Associate Professor with the School of Engineering, Edith Cowan University, Australia. His research interests include 5G technologies, green communications, QoS in communication networks, software-defined radio, wireless sensor networks, and computational intelligence.

**QUOC VIET PHUNG** (Member, IEEE) received the Ph.D. degree in communication engineering from Edith Cowan University, Australia, in 2010. He is currently a Lecturer with the School of Engineering, Edith Cowan University. His research interests include smart sensors, 5G technologies, underwater communication, software-defined radio, data analytics, network security, and applied artificial intelligence.

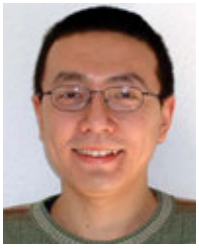

**YUE RONG** (Senior Member, IEEE) received the Ph.D. degree (summa cum laude) in electrical engineering from Darmstadt University of Technology, Darmstadt, Germany, in 2005. He was a Postdoctoral Researcher with the Department of Electrical Engineering, University of California at Riverside, Riverside, CA, USA, from February 2006 to November 2007. Since December 2007, he has been with Curtin University, Bentley, WA, Australia, where he is currently a Professor. His research interests include signal processing for communications, underwater acoustic communications, underwater optical wireless communications, machine learning, speech recognition, and biomedical engineering. He has published over 200 journal and conference papers in these areas.

**HAITHAM KHALED** received the Bachelor of Science degree in electrical and electronic engineering and the Master of Engineering and Ph.D. degrees from Edith Cowan University, Australia, in 2006, 2016, and 2021, respectively. He is currently a casual Lecturer with the School of Engineering, Edith Cowan University. His research interests include green communications, wireless networks, and the evolution of 5G technologies.

**DARYOUSH HABIBI** (Senior Member, IEEE) received the Bachelor of Engineering degree in electrical engineering (Hons.) and the Ph.D. degree from the University of Tasmania, in 1990 and 1995, respectively. He has over 200 refereed publications in journals, conference proceedings, and book chapters. His research interests include engineering design for sustainable development, renewable and smart energy systems, environmental monitoring technologies, and reliability and quality of service in engineering systems and networks. He is a fellow of Engineers Australia and the Institute of Marine Engineering, Science and Technology.